

Supporting Information

Teesalu et al. 10.1073/pnas.0908201106

SI Materials and Methods

Mice and Tissues. All animal experimentation was performed according to procedures approved by the Animal Research Committee at the University of California, Santa Barbara. Before tumor injections, other procedures, and killing, the mice were anesthetized with i.p. injections of xylazine (10 mg/kg) and ketamine (50 mg/kg). BALB/c athymic nude mice (Harlan Sprague–Dawley) were used for tumor xenografts and in vivo and *ex vivo* phage display experiments. Orthotopic prostate tumor xenografts were generated by injecting 10^6 PPC-1 cells (1) into the ventral lobe of the prostate. For histologic analysis, tissues were fixed in 4% paraformaldehyde, cryoprotected in PBS solution containing 30% sucrose, frozen, and sectioned at 10 μ m.

Cell Lines. PPC-1, PC-3, Du-145, F2, and M21 cell lines were cultured in DMEM supplemented with 10% FBS and penicillin/streptomycin.

Phage Display. The T7-select phage display system (EMD Biosciences) was used to construct phage libraries (diversity, 10^8) and individual phage cloning according to the manufacturer's instructions. Phage was purified by precipitation with PEG-8000 (Sigma) followed by CsCl_2 gradient ultracentrifugation and dialysis. The sequences of displayed peptides were determined from the DNA encoding the insert-containing region at the C terminus of the T7 major coat protein gp10.

For library screening and phage binding studies, cultured cells were grown to near-confluence and dissociated with trypsin, and mouse organs were dissociated using the Medimachine system (BD Biosciences). To measure phage binding, 10^6 cells in binding buffer (DMEM containing 1% BSA) were incubated with 10^9 pfu/mL of phage for 1 h at 4 °C. The cells were washed 4 times with the binding buffer, lysed in LB bacterial growth medium containing 1% Nonidet P-40, and phage was titrated. In some cases, phage particles (10^9 pfu) were treated with different concentrations of crystalline trypsin (Sigma) at 37 °C for 30 min. The proteolytic reaction was terminated with 5 mg/mL of soybean inhibitor before use in binding assays at 4 °C with a 3-h incubation.

Phage internalization assays used the same procedure, except that the cells were incubated with the phage at 37 °C and that an acidic buffer (500 mM sodium chloride, 0.1 M glycine, and 1% BSA, pH 2.5) was used instead of the binding buffer in the second wash to remove and inactivate the extracellular phage.

Potential inhibitors of phage binding and internalization (endocytosis inhibitors, free peptides, qdots, and UV-inactivated phage) were added to the cells 15–20 min before incubation with phage. Endocytosis inhibitors used in this study were the following: nystatin (50 μ g/mL), genistein (100 μ g/mL), chlorpromazine (5 μ g/mL), 5-(*N*-ethyl-*N*-isopropyl)amiloride (100 μ M), and wortmannin (10 μ M).

In vivo phage homing studies in mice were performed by injecting 10^{10} pfu of phage into tail vein, and 10 min to 1 h later the mice were perfused with DMEM through the left ventricle of the heart. The organs of interest were collected, homogenized in 1% Nonidet P-40, and the phage was quantified by titration.

Peptide Synthesis and Qdot Labeling. Peptides were synthesized using Fmoc/t-Bu chemistry on a microwave-assisted automated peptide synthesizer (Liberty; CEM Corporation). Peptides were purified by HPLC using 0.1% TFA in acetonitrile–water mixtures to 90–95% purity and validated by quadrupole TOF mass

spectral analysis. Streptavidin ITK-605 quantum dots (Invitrogen) were modified with biotinylated peptides by incubation with a 100-fold molar excess of peptide followed by removal of free peptide by dialysis.

Affinity Chromatography. Orthotopic PPC-1 tumors were homogenized in PBS containing 400 mM n-octyl-beta-D-glucopyranoside, 1 mM MgSO_4 , 1 mM MnCl_2 , 1 mM CaCl_2 , and a protease inhibitor mixture (Sigma). After 6 h of extraction on a rotating platform at 4 °C, the lysate was cleared by centrifugation (20 min at 22,000 $\times g$ at 4 °C) and loaded onto an affinity column prepared by coupling N-terminal cysteine-tagged RPARPAR peptide to Sulfolink coupling gel according to the manufacturer's instructions (Pierce). After overnight binding at 4 °C, the column was washed with extraction buffer containing 200 mM n-octyl-beta-D-glucopyranoside, followed by elution with 2 mM free RPARPAR peptide in the same buffer. Samples of the wash and elution fractions were separated using Novex 4–20% Tris-glycine polyacrylamide gels (Invitrogen), silver stained using the Silver Snap kit (Pierce), and subjected to MALDI-TOF mass spectrometry at the Burnham Institute for Medical Research Proteomics Facility. Affinity chromatography samples were separated by gel electrophoresis, immunoblotted, and probed with antibodies, followed by chemiluminescent detection.

Immunofluorescence Staining. Cells (2×10^5) were grown in 6-well tissue culture plates on collagen-I-coated coverslips (BD Biosciences) overnight at 37 °C in 5% CO_2 , and incubated with 10^8 pfu of phage. The cells were fixed in 4% paraformaldehyde or cold (–20 °C) methanol, and stained with antibodies. Nuclei were stained with DAPI or Hoechst 342. A polyclonal rabbit anti-T7 phage antibody was generated in house as by immunizing rabbits with CsCl_2 -purified phage. Other primary antibodies used were rat monoclonal antimouse CD31 antibody (BD Biosciences), rabbit anti-NRP-1, mouse antihuman Lamp-1, mouse antihuman caveolin (Millipore), mouse anti-NRP-1 (Miltenyi Biotec), and mouse antihuman EEA-1 (BD Biosciences). The secondary antibodies, Alexa594 goat antibodies to mouse, rat, and rabbit immunoglobulins and Alexa488 donkey antirabbit antibody, were from Invitrogen. Cells and tissue sections were examined by confocal microscopy (Fluoview 500; Olympus America).

DNA Constructs and Transfection. Expression construct of the wild-type NRP-1 cDNA in pcDNA3.1(+) was a kind gift from Dr. Michael Klagsbrun. Site-directed mutagenesis was used to generate triple mutation of the VEGF-165 binding site in the b1 domain of NRP-1 (S346A-E348A-349A; ref. 2) by replacing TCAAAAGAAACC (encoding amino acids SKET) with GCTAAAGCTGCT (encoding AKAA). M21 melanoma cells were transiently transfected with these constructs using lipofectamine according to the manufacturer's instructions (Invitrogen).

Extravasation and Tissue Penetration Assays. For modified Miles assay, anesthetized athymic nu/nu mice were injected i.v. with a 3-tracer mixture consisting of 0.5% Evans Blue, 13 μ g of Quantilum recombinant luciferase (Promega), and 10^9 pfu of phage particles in 150 μ L of PBS. Ten minutes later the mice were injected intradermally in 2 rows on the ventral skin with 40 μ L PBS containing either 50 ng VEGF, 500 μ M of peptide, tetrameric neutravidin–peptide complexes (Pierce; peptide con-

centration, 8 μM), or peptide complexes multimerized by coating Streptavidin ITK-605 qdots (Invitrogen) with biotinylated peptide (peptide concentration, 1.2 μM). Thirty minutes later the mice were killed by perfusion through the heart, and the skin in the injection area was removed and cleaned of subcutaneous connective tissue. Samples of skin (4 mm in diameter) were punched out from the injection sites and photographed for Evans blue uptake. The skin samples were then homogenized in a buffer containing 1% Nonidet P-40 and assayed for luciferase activity and phage titer. For antibody inhibition, 20 $\mu\text{g}/\text{mL}$ of blocking anti-NRP-1 antibody or PBS was injected 30 min before the Evans Blue/luciferase/phage tracer injection.

In a systemic leakage assay, BALB/c mice were injected i.v. with 200 μL of PBS containing multimeric peptide complexes prepared by binding a biotinylated peptide onto Streptavidin ITK-605 qdots (Invitrogen; peptide concentration, 2.4 μM) and 10^9 pfu of inert phage particles. After 30 min of circulation, mice were perfused with 20 mL of DMEM containing 1% BSA, organs were collected and homogenized in LB medium containing 1% Nonidet P-40, and the phage present were quantified by titration.

Affinity Measurements. Affinity of RPAPAR peptide for NRP-1 (R&D Systems) was quantified by measuring IC_{50} in an ELISA-based assay. First, saturation binding assays were performed. Microtiter wells coated with 5 $\mu\text{g}/\text{mL}$ of the purified protein were incubated for 1 h at room temperature with various concentrations of biotinylated RPAPAR peptide in PBS for NRP-1 binding. After washing with the same buffer added with 0.01% Tween 20, streptavidin-conjugated horseradish peroxidase (Vector Laboratories) was added to the wells and incubated for 30 min at room temperature. Horseradish peroxidase binding was quantified with 2,2-azino-bis(3-ethylbenzthiazoline-6-sulfonic acid) (Sigma) as a substrate. Next, various concentrations of nonlabeled test peptides and a biotinylated reporter peptide at a concentration that gave half-maximal binding were incubated in the coated wells. Affinities were determined as described in ref. 3.

Statistical Analysis. Data were analyzed by two-tailed Student's *t* test and 1-way ANOVA, followed by suitable post hoc test.

1. Zhang L, Giraudo E, Hoffman JA, Hanahan D, Ruoslahti E (2006) Lymphatic zip codes in premalignant lesions and tumors. *Cancer Res* 66:5696–5706.
2. Vander Kooi CW, et al (2007) Structural basis for ligand and heparin binding to neuropilin B domains. *Proc Natl Acad Sci USA* 104:6152–6157.
3. Müller R (1980) Calculation of average antibody affinity in anti-hapten sera from data obtained by competitive radioimmunoassay. *J Immunol Methods* 34:345–352.

Peptides recovered after ex vivo selections		
CX7C	X7	RXXRXXX
CSVIQRSPR	VVERVRR	RPVRTSR
CAPRTPR	DKDKPLR	R
PIPAR	GTWKQLR	RLSRNPR
CPR	AVRRSAR	RPTRMPR
CIKTAR	AKGRSPR	RGVR
CLQPR	ARVRGYR	RIRRTDR
CSGIR	RVGRGFR	RLQRVHR
CVRSPR	RTQR	RPARPAR
CRTVVR	SIRRTQR	RGERPPR
CNHGNRQQC	RSRTQSR	RVTRPPR

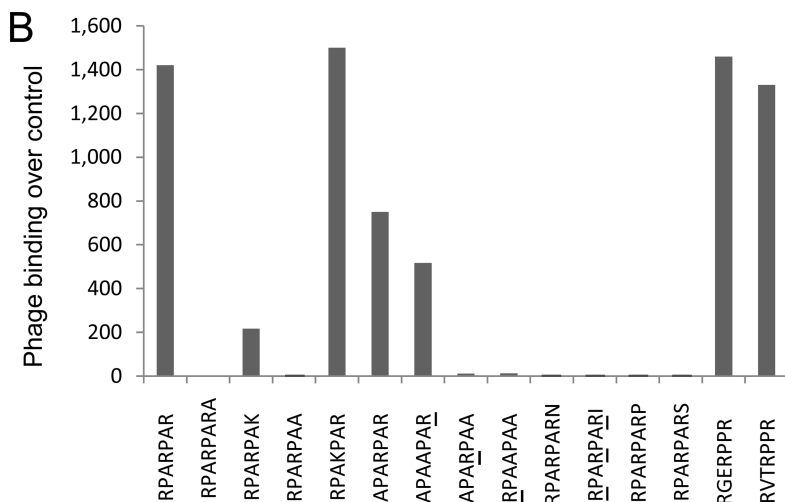


Fig. S1. Identification and characterization of CendR peptides. (A) Three peptide libraries (CX7C, X7, and RXXRXXX; C = cysteine; X = any amino acid) were used for ex vivo selection on cell suspensions derived from orthotopic PPC-1 xenograft tumors. Representative peptide sequences recovered after three rounds of ex vivo selections are shown. Peptides ending with C-terminal arginine comprised more than 90% of all phage inserts. (B) Binding of RPAPAR phage to cultured PPC-1 cells at 4 °C. The data are representative of 4 independent binding experiments. Binding is expressed as fold over control phage displaying polyvaline heptapeptide (G7). Arginines and lysines are shown with underbars.

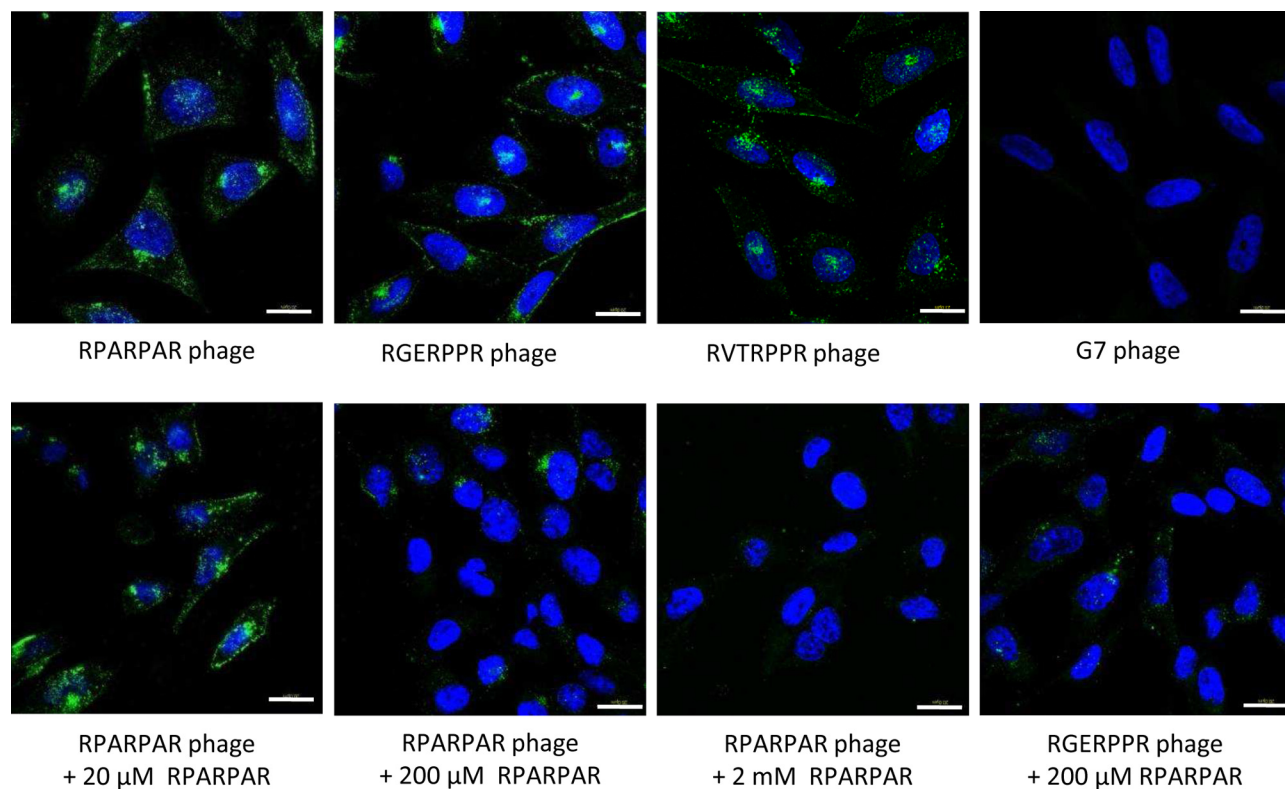


Fig. S2. Cellular binding and uptake of RPARPAR, RGERPPR, and RVTRPPR peptides: A shared pathway. Confocal immunofluorescence assessment of phage immunoreactivity (green) in PPC-1 cells cultured for 1 h in the presence of 10^9 pfu of the indicated phage. Where indicated, free RPARPAR peptide was added to the incubation media. Blue, DAPI. (Scale bars, 20 μ m.)

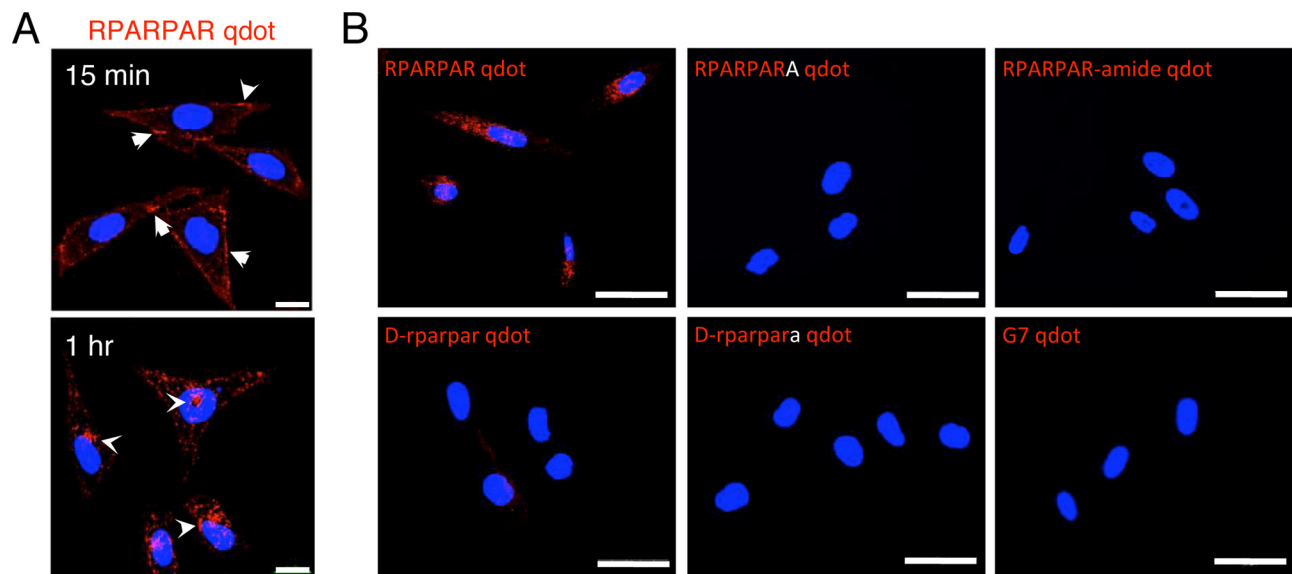


Fig. S3. Internalization of RPARPAR qdots by PPC-1 cells: Effect of peptide modification. (A) Internalization of RPARPAR qdots by live PPC1 cells at 37 °C. Fifteen minutes after the addition of the qdots, labeling is seen along the plasma membrane (*Top*, arrowheads). After 1 h, most of the qdots are internalized (*Bottom*, arrowheads). Nuclei were stained with an intravital nuclear stain (Hoechst 342). (Scale bars, 20 μm .) (B) PPC1 cells were incubated for 2 h with qdots functionalized with the indicated peptides. The lowercase letters refer to D-amino acids in the peptides. The cells were stained with nuclear stain DAPI and imaged using a confocal microscope. (Scale bars, 50 μm .)

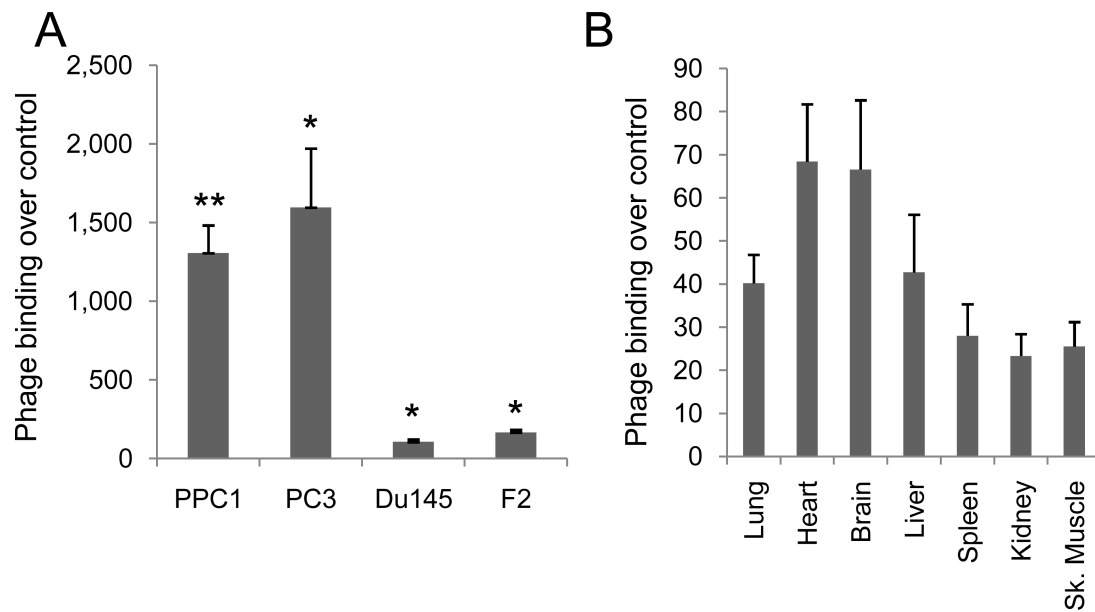


Fig. S4. CendR phage binds to different types of cells. (A) Binding of RPARPAR phage to cultured cells at 4°C. (B) Binding of RPARPAR phage to primary cell suspensions from mouse organs at 4°C. The titer of RPARPAR phage is expressed as fold over control G7 phage. Statistical analysis was performed by Student's *t* test. *n* = 3; error bars indicate SEM; *, *P* < 0.05; **, *P* < 0.01.

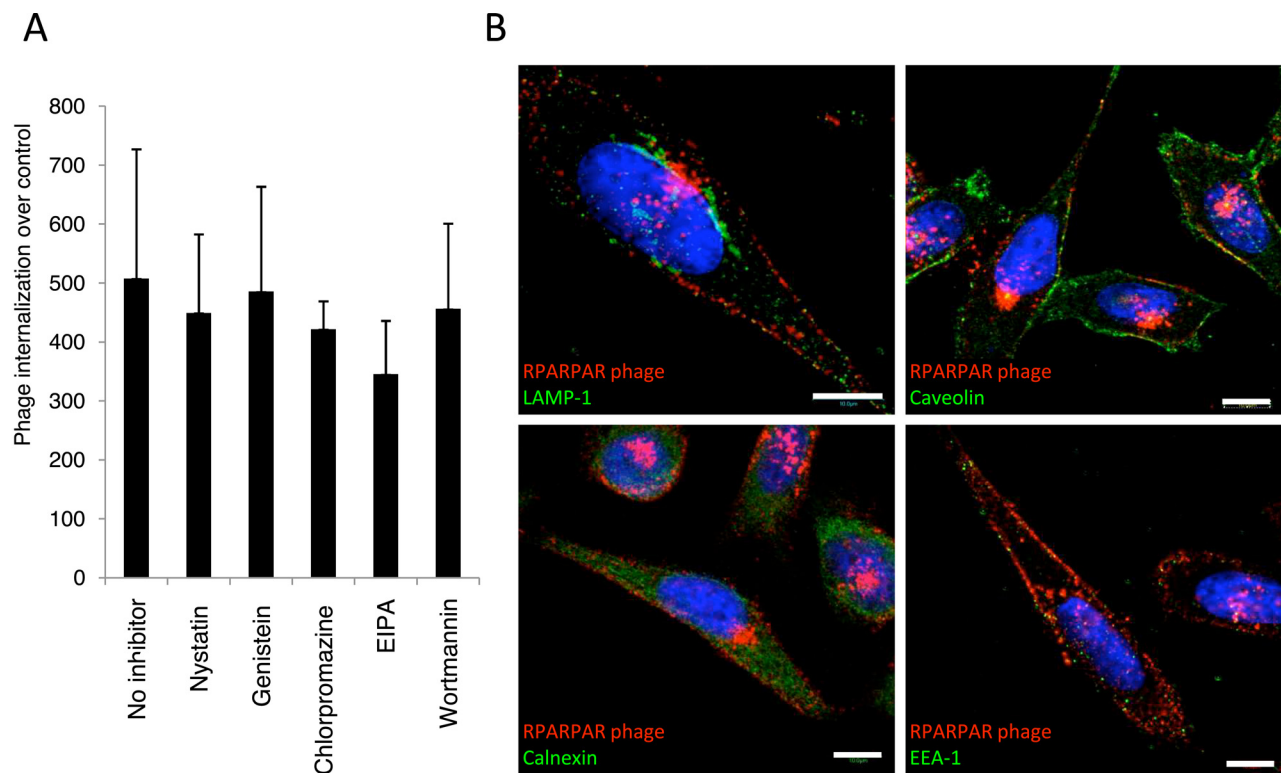


Fig. S5. RPAPAR phage is internalized into PPC-1 cells via an unconventional pathway. (A) Effect of endocytosis inhibitors on RPAPAR phage internalization. Phage was incubated with PPC1 cells in the presence of the indicated inhibitor compounds for 90 min at 37 °C, followed by acid wash and titration to quantify the internalized phage. Statistical analysis (performed by ANOVA) showed that none of the compounds significantly inhibited the internalization. $n = 3$; error bars indicate SEM. (B) Confocal imaging of PPC1 cells incubated for 60 min in the presence of 10^9 pfu of RPAPAR phage and double stained for phage (red) and subcellular compartment markers (green; LAMP-1, caveolin-1, calnexin, or EEA-1). Nuclei were stained with DAPI. (Scale bars, 10 μ m.)

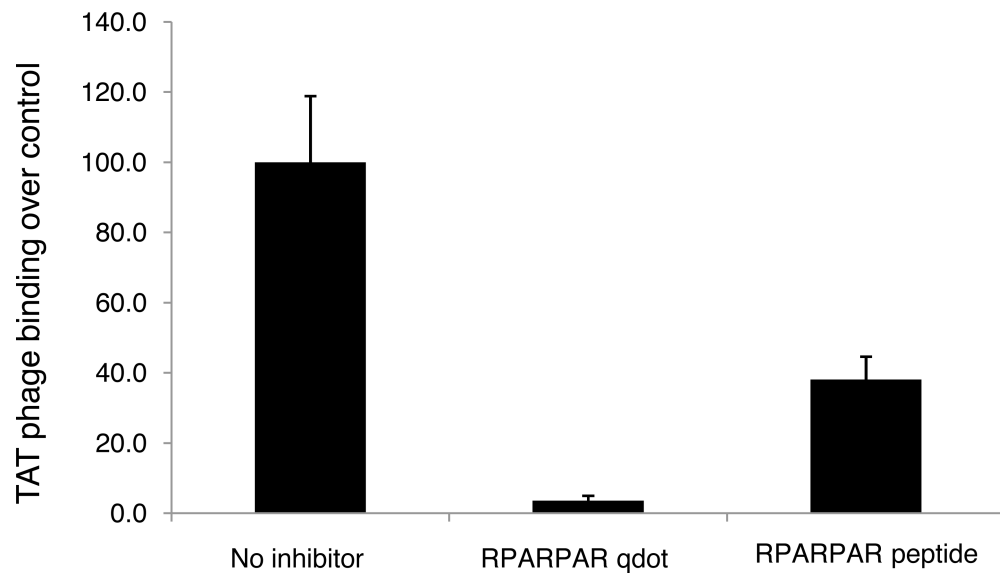


Fig. S6. Inhibition of the binding of phage displaying the TAT peptide (RKKRRQRRR) to PPC-1 cells. PPC-1 cells were incubated with DMEM containing 10^8 pfu of phage displaying the TAT peptide at 4°C for 60 min, followed by repeated washing with DMEM and titration of bound phage. In inhibition experiments, phage incubation was preceded by a 15-min incubation with DMEM containing 4 nM qdots or 200 μM peptide; the inhibitors were also added to the phage incubation buffer. $n = 3$; error bars indicate SEM.

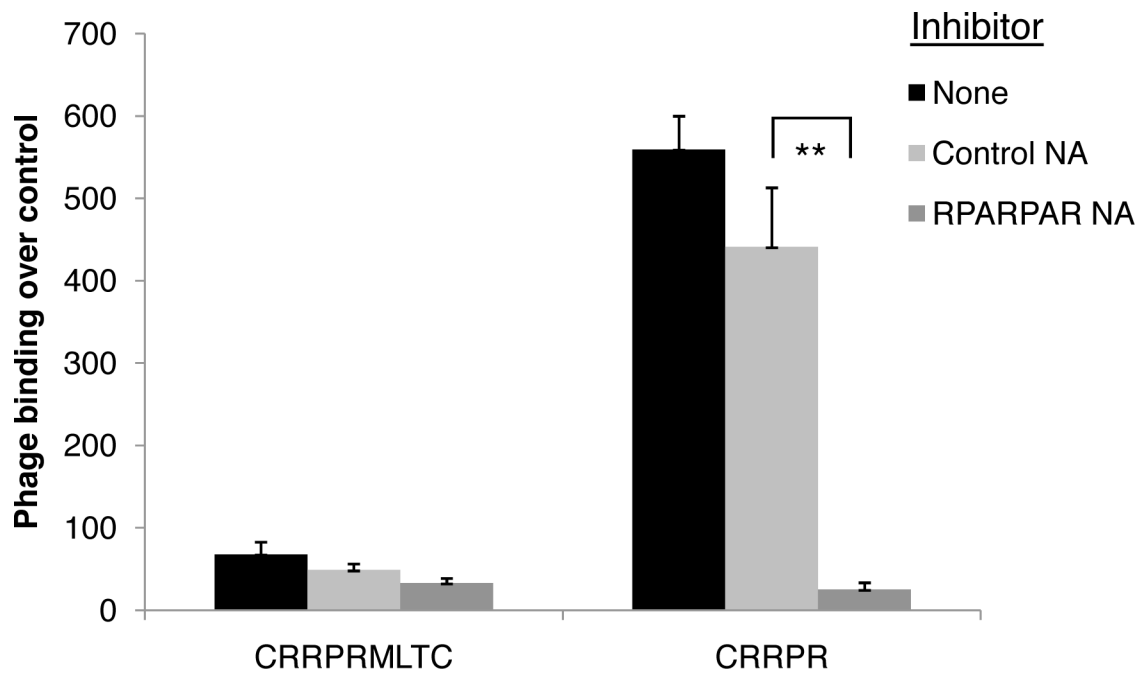


Fig. S7. Binding of CRRPRMLTC and CRRPR peptides of PPC-1 cells. PPC1 cells were incubated with DMEM containing 10^8 pfu of phage displaying either intact CRRPRMLTC or its derivative with exposed C-terminal CendR elements, CRRPR. The incubation was done at 4°C for 60 min, followed by repeated washing with DMEM and titration of bound phage in inhibition experiments, phage incubation was preceded by a 15-min incubation with DMEM containing no additions, or 100 nM control or RPARPAR neutravidin (NA); the inhibitors were also added to the phage incubation buffer. Statistical analysis was performed by Student's *t* test. $n = 3$; error bars indicate SEM; **, $P < 0.01$.

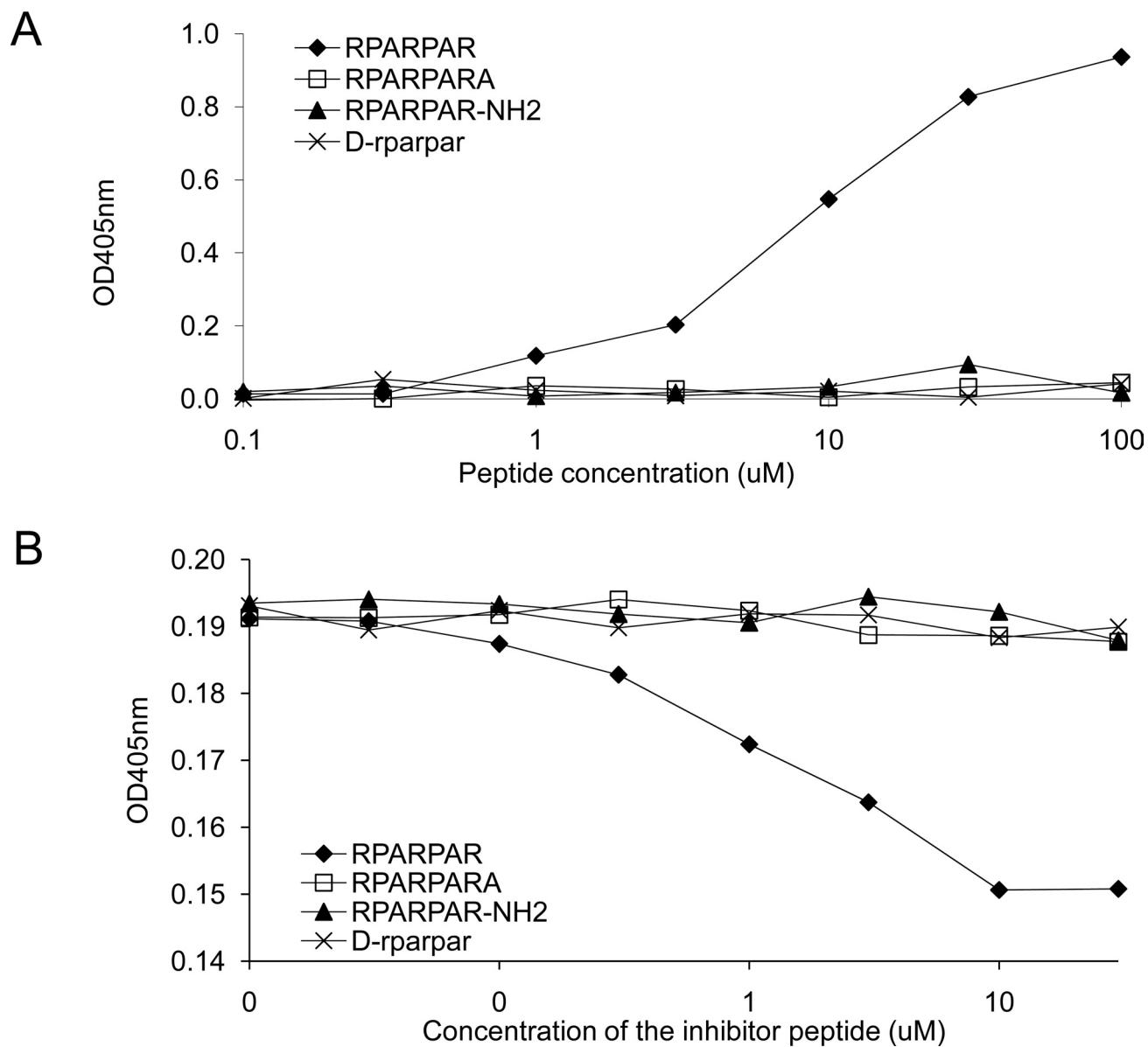


Fig. S8. NRP-1-binding affinity of RPARPAR and its variants. (A) Saturation binding of biotinylated RPARPAR peptide and the indicated variants of this peptide to purified NRP-1 immobilized on microtiter wells. The binding was detected with streptavidin coupled to horseradish peroxidase. The RPARPAR peptide concentration that gave half-maximal binding ($9.7 \mu\text{M}$) was used in subsequent inhibition assays shown in panel B. (B) NRP-1 binding of biotinylated RPARPAR peptide in the presence of increasing concentration of nonlabeled RPARPAR peptide and its variants. A $K_d = 1.7 \mu\text{M}$ for the NRP-1-RPARPAR interaction was determined from the inhibition data as described previously (3).

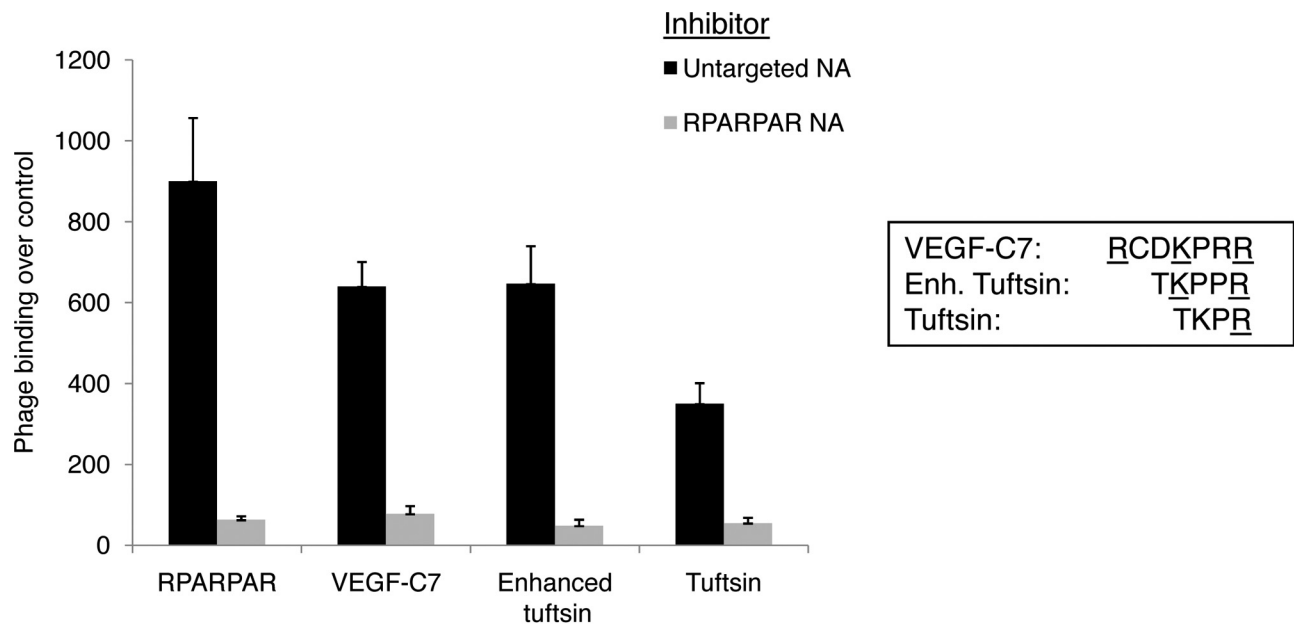


Fig. S9. Oligomeric RPARPAR peptide inhibits binding of phage displaying known NRP-1 ligand peptides to PPC-1 cells. PPC1 cells were incubated with DMEM containing 10^8 pfu of phage displaying the indicated peptides at 4 °C for 60 min, followed by repeated washing with DMEM and titration of bound phage. In inhibition experiments, phage incubation was preceded by a 15-min incubation with DMEM containing 100 nM control or RPARPAR neutravidin (NA); the inhibitors were also added to the phage incubation buffer. $n = 3$; error bars indicate SEM.

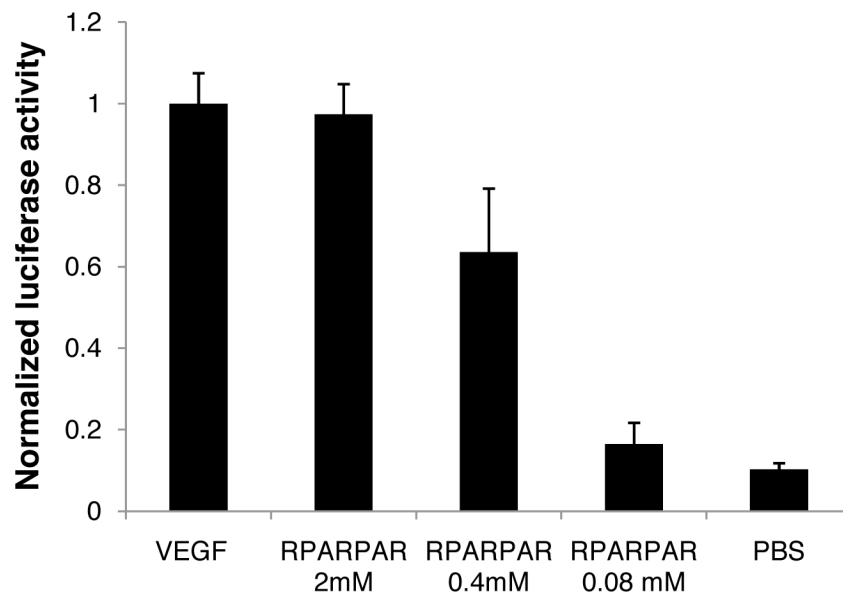


Fig. S10. Monomeric CendR peptides cause vascular leakage. Miles assay was performed by injecting luciferase i.v., followed by intradermal injections of 50 ng VEGF-165 or various amounts of RPAPAR peptide in 40 μ L of PBS, or PBS alone. Luciferase activity in VEGF-injected skin was set to equal 1.

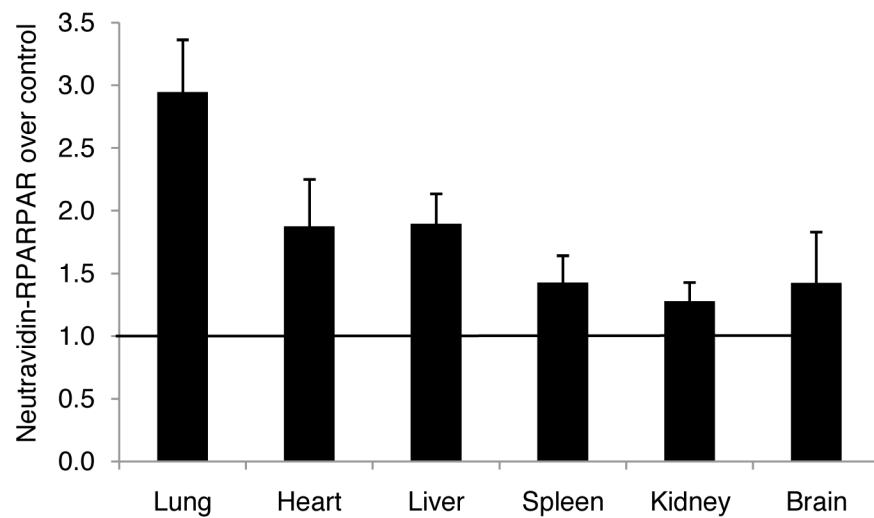


Fig. S11. Systemic injection of oligomeric RPARPAR peptide increases tissue retention of tracer phage. Mice were injected i.v. with 150 μ L of PBS containing 10^{10} pfu of a mixture of phage with an inactive insert (G7) and 8 μ M biotinylated RPARPAR (or control) peptide oligomerized using tetrameric neutravidin as a scaffold. After 30 min of circulation, mice were perfused through the heart, and retention of phage in tissues was determined by titration. The values on the y axis represent RPARPAR/control ratio. $n = 3$; error bars indicate SEM.

Virus	Protein	Sequence [* : cleavage site]	Reference
Human cytomegalovirus	Envelope glycoprotein B (UL55)	LNITH RTRR *STSDN	(1)
Measles virus	Fusion protein	SVASSR RHKR *FAGVV	(2)
Tick-born encephalitis virus	PreM protein	KQEGSR TRRR *SVLIP	(3)
Respiratory syncytial virus	Fusion protein	PATNN RAARR *ELPRF	(4)
Influenza A virus (H5N1)	Hemagglutinin	PQRERR RRKKR *GLFGA	(5)
HIV-1	Envelope precursor gp160	RRVVQ REKR *AVGIG	(6)
Zaire ebolavirus	Virion spike glycoprotein precursor	LITGG RRTR *REAIV	(7)
Mumps virus	Fusion protein	PSSGSR RHKR *FAGIA	(8)
Yellow fever virus	PreM protein	CDSAGR SRRR *SRRAI	(9)
Human herpesvirus 4	BALF4 (glycoprotein B)	AAVL RRRR *RDAGN	(10)
Human metapneumo-virus	Fusion glycoprotein precursor	QIENP RQSR *FVLGA	(11)
Human T-lymphotropic virus-2	Env propeptide	PPPAT RRRR *AVPIA	(12)
Crimean-Congo hemorrhagic fever virus	Glycoprotein precursor	PSPTN RSKR *NLKME	(13)

1. Vey M, et al. (1995) Proteolytic processing of human cytomegalovirus glycoprotein B (gpUL55) is mediated by the human endoprotease furin. *Virology* 206:746–749.
2. Varsanyi TM, Jorvall H, Norrby E (1985) Isolation and characterization of the measles virus F1 polypeptide: comparison with other paramyxovirus fusion proteins. *Virology* 147:110–117.
3. Chambers TJ, et al. (1990) Evidence that the N-terminal domain of nonstructural protein NS3 from yellow fever virus is a serine protease responsible for site-specific cleavages in the viral polyprotein. *Proc Natl Acad Sci USA* 87:8898–8902.
4. González-Reyes L, et al. (2001) Cleavage of the human respiratory syncytial virus fusion protein at two distinct sites is required for activation of membrane fusion. *Proc Natl Acad Sci USA* 98:9859–9864.
5. Steinhauer DA (1999) Role of hemagglutinin cleavage for the pathogenicity of influenza virus. *Virology* 258:1–20.
6. Moulard M, Decroly E (2000) Maturation of HIV envelope glycoprotein precursors by cellular endoproteases. *Biochim Biophys Acta* 1469:121–132.
7. Wool-Lewis RJ, Bates P (1999) Endoproteolytic processing of the ebola virus envelope glycoprotein: Cleavage is not required for function. *J Virol* 73:1419–1426.
8. Elango N, Varsanyi TM, Kövamees J, Norrby E (1989) The mumps virus fusion protein mRNA sequence and homology among the paramyxoviridae proteins. *J Gen Virol* 70:801–807.
9. Ruiz-Linares A, Cahour A, Després P, Girard M, Bouloy M (1989) Processing of yellow fever virus polyprotein: Role of cellular proteases in maturation of the structural proteins. *J Virol* 63:4199–4209.
10. Johannsen E, et al. (2004) Proteins of purified Epstein-Barr virus. *Proc Natl Acad Sci USA* 101:16286–16291.
11. Biacchesi S, et al. (2006) Modification of the trypsin-dependent cleavage activation site of the human metapneumovirus fusion protein to be trypsin independent does not increase replication or spread in rodents or nonhuman primates. *J Virol* 80:5798–5806.
12. Sjöberg M, Wallin M, Lindqvist B, Garoff H (2006) Furin cleavage potentiates the membrane fusion-controlling intersubunit disulfide bond isomerization activity of leukemia virus Env. *J Virol* 80:5540–5551.
13. Sanchez AJ, Vincent MJ, Erickson BR, Nichol ST (2006) Crimean-congo hemorrhagic fever virus glycoprotein precursor is cleaved by Furin-like and SKI-1 proteases to generate a novel 38-kilodalton glycoprotein. *J Virol* 80:514–525.